

**THE EFFECT OF GOLD NANOPARTICLE SIZE  
IN BREAST CANCER MCF-7 CELL LINE  
TREATMENT BY X-RAY AND  
LINEAR ACCELERATOR (LINAC)**

**NUR SHAFAWATI BINTI ROSLI**

**UNIVERSITI SAINS MALAYSIA  
2017**

**THE EFFECT OF GOLD NANOPARTICLE SIZE  
IN BREAST CANCER MCF-7 CELL LINE  
TREATMENT BY X-RAY AND  
LINEAR ACCELERATOR (LINAC)**

by

**NUR SHAFAWATI BINTI ROSLI**

**Thesis submitted in fulfillment of the requirements for  
the degree of  
Doctor of Philosophy**

**May 2017**

## ACKNOWLEDGEMENT

In the name of Allah, the most gracious, the most merciful. In the 2012 until 2017 that this research, or portions of it, has been in preparation, the list of persons to whom I am indebted for assistance, criticism, and encouragement has grown to unmanageable proportions. I hope I will be pardoned for singling out a few upon whom I have called most frequently for help, and failing to name many others who have aided me. First of all, I wish to express my gratitude to my supervisor, Dr. Azhar bin Abdul Rahman, who was abundantly helpful and offered invaluable assistance, support and guidance. I am also indebted to Prof. Dr. Azlan bin Abdul Aziz and Prof. Dr. Shaharum bin Shamsuddin as my co-supervisors for their encouragement, guidance and support from the initial to the final level enabled me to develop an understanding of the subject, the materials provided in preparing this research and for their assistance in preparing the manuscript. I am heartily thankful to Puan Nor Dyana Zakaria, Research Officer of NanoBiotechnology Research and Innovation (NanoBRI), Institute for Research in Molecular Medicine (INFORMM), Universiti Sains Malaysia for his kindness co-operation for giving permission to complete my labwork there. Special thanks go to Mr. Ng Boon Seng, Chief Medical Physicist (Radiotherapy and X-Ray), Pantai Hospital Penang, and his staff Azean for their kindness co-operation for giving permission to use the LINAC to complete my data collection there and assists me in processing and collecting data from the beginning and to the final stage. Without their knowledge and assistance this study would not have been successful. Their timeless and tireless effort is very much appreciated.

I would like to take this opportunity to thank Malaysian government for awarding me MyBrain15 (MyPhD) scholarship. Grateful acknowledgement is also made here to Universiti Sains Malaysia through USM Short Term Grant (304/PFIZIK/6312104) for the funding of this research. I am also indebted to the School of Physics, University Sains Malaysia, for the support and trust given to me in preparing the research entitled “The Effect of Gold Nanoparticle Size in Breast Cancer MCF-7 Cell Line Treatment By X-Ray and Linear Accelerator (LINAC)” in fulfillment of requirements for the degree of Doctor of Philosophy in School of Physics, Universiti Sains Malaysia. This research project would not have been possible without the support of many people. Special thanks also to all my postgraduate friends, for sharing the literature, invaluable assistance and always being there. I hasten to pronounce the customary absolution, relieving all the persons mentioned above of responsibility for what I have written; but I cannot absolve them of responsibility for providing the source inspiration from which the research was drawn. And finally, I wish to express my love and dedicated this research to my beloved husband, Khairul Anwar Mohd Yusof and my family, especially to my parents, Rosli bin Omar and Asmah Wan Chik, whose patience and resourcefulness allowed me to concentrate on writing it, and whose cheerfulness and support were a constant inspiration for their understanding and endless love, through the duration of my study. Without their encouragement, I would not have finished this study. There are not enough words to describe my boundless gratitude to all of you. Thank you.

## TABLE OF CONTENTS

<b>ACKNOWLEDGEMENT</b>	ii
<b>TABLE OF CONTENTS</b>	iv
<b>LIST OF TABLES</b>	viii
<b>LIST OF FIGURES</b>	ix
<b>LIST OF ABBREVIATIONS</b>	xii
<b>ABSTRAK</b>	xiv
<b>ABSTRACT</b>	xvi
<b>CHAPTER 1 - INTRODUCTION</b>	
1.0 Introduction	1
1.1 Background of Study	1
1.2 Problem Statement	4
1.3 Objectives	7
1.4 Significance of Study	7
1.5 Outline of Thesis	8
<b>CHAPTER 2 - BACKGROUND, THEORY AND LITERATURE</b>	
<b>REVIEW</b>	
2.0 Introduction	10
2.1 Gold Nanoparticles	10
2.1.1 Synthesis	11
2.1.2 Chemical Properties	11

2.1.3	Physical Properties	12
2.2	Basic Radiation Physics	15
2.3	AuNPs Radiation Therapy in the Kilovoltage Range	18
2.4	Interaction of Radiation with AuNPs at the Atomic Level	20
2.4.1	Coherent Scattering	21
2.4.2	Photoelectric Effect	22
2.4.3	Compton Scattering	24
2.4.4	Pair Production	25
2.5	AuNPs Radiosensitisation in Cell Line ( <i>In Vitro</i> ) and Animal Models ( <i>In Vivo</i> )	27
2.5.1	Radiation Damage	30
2.5.2	Cell Survival Curve	32
2.5.3	Linear-Quadratic Model	36
2.5.4	Linear Energy Transfer and Relative Biological Effectiveness	37
2.5.5	Cell Cycle Effects	41

### **CHAPTER 3 - MATERIALS AND METHODS**

3.0	Introduction	45
3.1	Preparation and Characterization of AuNPs for Experimental Use	45
3.2	Basic Cell Culture Protocol	48
3.2.1	Complete Media Preparation	48
3.2.2	Thawing Frozen Cells	50
3.2.3	Trypsinisation of Anchorage Dependent Cell	51

3.2.4	Cell Counting and Evaluation of Viable Cells	52
3.2.5	Cryopreservation Process	53
3.3	Cytotoxicity Test	54
3.3.1	Cell Morphology Analysis	54
3.3.2	Preparation of the MCF-7 Cells for the Cytotoxicity Test	55
3.3.3	Cytotoxicity of AuNPs on MCF-7 Cells	55
3.4	TEM Analysis of Cells with Internalized AuNPs	57
3.4.1	Cell Uptake and Fixation Preparation	57
3.4.2	Sample Preparation	58
3.4.3	Sectioning and Ultramicrotomy	60
3.4.4	Staining Cells and Viewing Process	63
3.5	Cell Irradiation	66
3.5.1	Kilovoltage Superficial X-Rays Radiotherapy	66
3.5.2	Megavoltage Photon Beams Radiotherapy	68

## **CHAPTER 4 - RESULTS AND DISCUSSIONS**

4.0	Introduction	70
4.1	Characterisation of AuNPs	70
4.1.1	Estimating the AuNPs Size via Zetasizer Particle Electrophoresis Instrument	70
4.1.2	Determining the Absorbance Properties of AuNPs via UV–vis–NIR Spectrophotometer	72
4.1.3	Characterizing the Size, Shape, and Morphology of AuNPs via TEM Imaging	74

4.2	Cell Morphology Analysis	74
4.2.1	Morphological Examinations by Inverted Microscope	75
4.3	Cytotoxicity of AuNPs on MCF-7 Cells	77
4.4	EFTEM Analysis of MCF-7 Cells with Internalized AuNPs	82
4.5	Cell Irradiation	88
4.5.1	Kilovoltage Superficial X-Rays Radiotherapy	88
4.5.2	Megavoltage Photon Beams Radiotherapy	93

## **CHAPTER 5 - CONCLUSION AND RECOMMENDATION**

5.0	Introduction	103
5.1	Conclusion	103
5.2	Recommendation for Further Work	107

<b>REFERENCES</b>	109
-------------------	-----

## **APPENDICES**

## **LIST OF PUBLICATIONS**



## LIST OF TABLES

	<b>Page</b>
Table 2.1 Bulk Properties of Gold Nanoparticles	14
Table 2.2 Subcategories of the X-ray therapy in the kilovoltage range based on the beam quality and their use.	19
Table 4.1 The maximum wavelength and absorption spectra of AuNPs.	73
Table 4.2 The survival fraction of MCF-7 cells when irradiated with 80 kVp and 20 mAs X-ray beams.	92
Table 4.3 The survival fraction of MCF-7 cells when irradiated with 6 MV photon beams.	96
Table 4.4 The survival fraction of MCF-7 cells when irradiated with 10 MV photon beams.	100

## LIST OF FIGURES

	<b>Page</b>
Figure 2.1	Mechanism of bremsstrahlung process. 16
Figure 2.2	Mechanism of characteristic radiation. 17
Figure 2.3	Mechanism of coherent scattering. 22
Figure 2.4	Mechanism of photoelectric effect. 23
Figure 2.5	Mechanism of compton effect. 24
Figure 2.6	Mechanism of pair production. 26
Figure 2.7	Mechanisms of radiation induces DNA damage. 31
Figure 2.8	Mechanisms of radiation induces DNA damage with the presence of AuNPs. 32
Figure 2.9	Shape of cell survival curve. 34
Figure 2.10	Shape of cell survival curve. The experimental data are fitted to a linear-quadratic function and the dose at which the linear and quadratic components are equal is the ratio $\alpha/\beta$ . 37
Figure 2.11	A diagrammatic view of the cell cycle. 43
Figure 3.1	The sample of spherical AuNPs (13 nm, 50 nm, and 70 nm) obtained in a liquid suspension. 46
Figure 3.2	The dispersity of the AuNPs was characterised by using a Zetasizer particle electrophoresis instrument (Nanoseries Model ZEN3600, Malvern Instruments). 46
Figure 3.3	The maximum wavelength and absorption spectra of AuNPs were determined by using UV-Vis NIR Spectrophotometer (Model UV-3600, Shimadzu) in the range of 400 to 800 nm. 48
Figure 3.4	Design of the experiment for all parts of the basic cell culture work. 49
Figure 3.5	Complete media of DMEM in a sterile bottle. 50
Figure 3.6	A sample of MCF-7 cell culture in 25 cm <sup>2</sup> flask. 51

Figure 3.7	The sample of MCF-7 cell culture in cryovials.	54
Figure 3.8	Cell morphology analysis by using; (A) XE-Bio Atomic Force Microscopy (Park System) and (B) Axio Observer Inverted Microscope (Carl Zeiss).	54
Figure 3.9	Schematic diagram of dilution of AuNPs in 96-well plate.	56
Figure 3.10	The specimen cubes of solidified agar containing the MCF-7 cells, and MCF-7 cells treated with 13 nm, 50 nm, and 70 nm AuNPs; (A) the specimen cubes were dehydrated in ethanol; (B) the specimen cubes were embed in resin mixture and cure at 60°C for 12 – 48 hours.	60
Figure 3.11	Schematic diagram of sample preparation.	61
Figure 3.12	The process of sectioning and ultramicrotomy; (A) Rough trimming was done by using razor blades; (B) Fine trimming was done by using the glass knives; (C) The knife-boats, which was filled with water, and the parallelness and distance of the “knife to block” was adjusted on the cutting microscope.	62
Figure 3.13	Ultra-thin sectioning process; (A) The colour scale for section thickness; (B) The sections which are gold or silver in colour were collected and put on the copper grids.	63
Figure 3.14	The cells are view under the Energy-Filtered Transmission Electron Microscope (EFTEM) Libra 120.	64
Figure 3.15	Schematic diagram of sectioning, ultramicrotomy, staining cells, and viewing process.	65
Figure 3.16	The set up for calibration of X-ray machine by using ionization chamber.	67
Figure 3.17	The set up for cell irradiation with megavoltage X-ray from clinical LINAC. Build up were placed on top on the plate to ensure maximum dose to the cells. Also, the cell medium was filled to reduce the air gap effects.	69
Figure 4.1	The graph of size distribution by intensity for 13 nm, 50 nm, and 70 nm AuNPs sample.	71
Figure 4.2	UV-Vis spectra of 13, 50 and 70 nm AuNPs.	72
Figure 4.3	TEM image of AuNPs with (A) 13 nm, (B) 50 nm and (C) 70 nm diameter of sizes at 380 000x magnification.	75

Figure 4.4	Morphological aspect of MCF-7 cells observed by (A) XE-Bio Atomic Force Microscopy (Park System) and (B) Axio Observer Inverted Microscope (Carl Zeiss).	76
Figure 4.5	Inverted microscope images of morphological changes on MCF-7 treated with (A) control; (B) 13 nm AuNPs; (C) 50 nm AuNPs; and (D) 70 nm AuNPs. Images are at 10 X magnification.	77
Figure 4.6	The graph shows cytotoxicity of 13 nm, 50 nm, and 70 nm gold nanoparticles in MCF-7 cell line.	78
Figure 4.7	Size-dependent cell uptake. (A) Cell uptake of NPs smaller than optimal size. (B) Cell uptake of optimal size NPs, 50 nm. (C) Cell uptake of NPs larger than optimal size.	80
Figure 4.8	Concentration-dependent cell uptake. (A) Cellular uptake of low concentration NPs. (B) Cellular uptake of high concentration NPs.	82
Figure 4.9	Energy-filtered transmission electron photomicrograph of control (A and B) or 13 nm AuNPs treated (C and D), MCF-7 cells cultured in complete media DMEM.	84
Figure 4.10	Energy-filtered transmission electron photomicrograph of 50 nm AuNPs treated (E and F), or 70 nm AuNPs treated (G and H), MCF-7 cells cultured in complete media DMEM.	85
Figure 4.11	Schematic diagram of the mechanism of nanoparticles cellular uptake; 1. NPs bound to membrane receptors; 2. Endocytosis of NPs; 3. NPs localized in endosomes; 4. Fusion of endosomes with lysosomes; 5. NPs localized in lysosomes; 6. Exocytosis of NPs.	87
Figure 4.12	Survival curves of MCF-7 cells when irradiated with 80 kVp and 20 mAs X-ray beams.	90
Figure 4.13	Survival curves of MCF-7 cells when irradiated with 6 MV photon beams.	94
Figure 4.14	Survival curves of MCF-7 cells when irradiated with 10 MV photon beams.	99

## LIST OF ABBREVIATIONS

AuNPs	Gold Nanoparticles
CFU	Colony Forming Unit
DMEM	Dulbecco's Modified Eagle's Medium
DMF	Dose Modifying Factor
EFTEM	Energy-Filtered Transmission Electron Microscope
FBS	Fetal Bovine Serum
HVL	Half Value Layer
IAEA	International Atomic Energy Agency
ICRP	International Commission on Radiological Protection
ICRU	International Commission on Radiation Units and Measurements
IGRT	Image-Guided Radiotherapy
IMRT	Intensity Modulated Radiotherapy
LET	Linear Energy Transfer
LINAC	Linear Accelerator
LQ	Linear-Quadratic
MCF-7	Michigan Cancer Foundation-7
NCRP	National Council on Radiation Protection
PBS	Phosphate Buffered Saline
PES	Polyethersulfone
PLD	Potentially Lethal Damage
RBE	Relative Biological Effectiveness
rpm	rotation per minute

SPA	Surface Plasmon Absorption
SRS	Stereotactic Radiosurgery
SSD	source to surface distance
TEM	Transmission Electron Microscope
Z	Atomic Number

**KESAN SAIZ NANOPARTIKEL EMAS DALAM RAWATAN  
KANSER PAYUDARA SEL MCF-7 MELALUI SINAR-X DAN  
PEMECUT LINEAR (LINAC)**

**ABSTRAK**

Partikel nano emas (AuNPs) telah digunakan untuk mempertingkatkan kesan radiasi dalam sel induk kanser payudara MCF-7 dengan peralatan radioterapi. AuNPs boleh digunakan dalam terapi sinaran bagi membunuh sel-sel kanser di samping mengurangkan dos radiasi yang diperlukan untuk membunuh tumor tersebut dan pada masa yang sama menyelamatkan tisu normal. Sinaran yang dilakukan menggunakan sinar-X kilovoltan ultra-permukaan dan pancaran foton megavoltan dalam radioterapi melalui mesin sinar-X dan pemecut linear (LINAC). Dalam projek ini, sel-sel MCF-7 dibiakkan di dalam plat 96-perigi dan dirawat dengan tiga saiz yang berbeza daripada partikel nano emas (13 nm, 50 nm, dan 70 nm) sebelum ianya disinari dengan pancaran sinar-X 80 kVp dan 20 mAs, dan pancaran foton 6 MV dan 10 MV di pelbagai dos radiasi. Untuk mengesahkan kesan kematian dipertingkatkan, kedua-dua sel MCF-7, iaitu dengan dan tanpa AuNPs, disinari secara serentak. Kemudian, sel-sel MCF-7 yang telah disinari akan disimpan di dalam inkubator pada suhu 37 °C dan 5 % CO<sub>2</sub> dalam atmosfera kelembapan selama 24 jam. Kuantiti sel-sel yang telah disinari dikesan dengan analisis yang menggunakan pembiakan sel WST-1 24 jam selepas penyinaran dan pecahan sel yang hidup tersebut kemudiannya dikira. Keputusan menunjukkan AuNPs secara ketara meningkatkan kadar pembunuhan sel kanser dengan mengurangkan pecahan sel yang hidup tersebut. Ini bermakna, AuNPs meningkatkan kesan radiasi kepada

sel-sel tersebut samada bagi penyinaran dengan sinar-X kilovoltan ultra-permukaan, atau pancaran foton megavoltan dalam radioterapi. Selain itu, lengkuk sel yang hidup yang diperolehi juga menyokong kuat hujah bahawa saiz AuNPs juga memainkan peranan yang penting dalam menentukan peningkatan kesan radiasi. Berdasarkan lengkuk sel MCF-7 yang hidup, ianya jelas menunjukkan bahawa 50 nm AuNPs membunuh lebih sel-sel MCF-7 dan menghasilkan pecahan yang hidup lebih rendah berbanding 13 nm dan 70 nm AuNPs. Nilai pecahan yang hidup bagi sel-sel MCF-7 yang dirawat dengan 50 nm AuNPs jelas menunjukkan ianya jauh lebih rendah berbanding nilai pecahan yang hidup sel-sel MCF-7 yang dirawat dengan 13 nm dan 70 nm AuNPs yang diperolehi dengan pancaran sinar-X 80 kVp, dan pancaran foton 6 MV dan 10 MV. Kesimpulannya, AuNPs boleh digunakan semasa terapi radiasi untuk membunuh sel-sel kanser di samping mengurangkan dos sinaran untuk membunuh sel-sel kanser dan pada masa yang sama menyelamatkan tisu normal.



**THE EFFECT OF GOLD NANOPARTICLE SIZE IN  
BREAST CANCER MCF-7 CELL LINE TREATMENT BY X-RAY AND  
LINEAR ACCELERATOR (LINAC)**

**ABSTRACT**

Gold Nanoparticles (AuNPs) has been used to enhance the radiation effects in MCF-7 breast adenocarcinoma cell line by radiotherapy equipments. AuNPs can be used during radiation therapy to kill cancer cells in order to reduce the dose of radiation to kill the tumours, while at the same time sparing the normal tissue. The irradiation were done using superficial kilovoltage X-rays and megavoltage photon beams in radiotherapy which are via X-ray machine and Linear Accelerator (LINAC). In this work, MCF-7 cells are seeded in the 96-well plate and were treated with three different sizes of AuNPs (13 nm, 50 nm, and 70 nm) before they were irradiated with 80 kVp and 20 mAs X-ray beams, 6 MV, and 10 MV photon beam at various radiation doses. To validate the enhanced killing effect, both with and without AuNPs MCF-7 cells is irradiated simultaneously. Then, the irradiated MCF-7 cells were incubated at 37 °C and 5% CO<sub>2</sub> in a humidified atmosphere incubator for 24 hours. The absorbance of the irradiated cells were detected with WST-1 cell proliferation assay 24 hours after irradiation and then, the cell survival fractions were calculated. The results show that AuNPs significantly enhance cancer killing by reducing the survival fraction of the cell. Means that, AuNPs enhance the radiation effects to the cells in either irradiation with kilovoltage superficial X-rays, or megavoltage photon beams radiotherapy. Additionally, the obtained cell survival curves also lend a strong support to the argument that the size of AuNPs also plays

important role in determining the enhancement radiation effects. Based on the survival curves of MCF-7 cells, it is clearly shows that 50 nm AuNPs kill the MCF-7 cells more and give the lower survival fraction compared to 13 nm and 70 nm AuNPs. The survival fraction value of MCF-7 cells treated with 50 nm AuNPs clearly shows that it is significantly lower than survival fraction value of MCF-7 cells treated with 13 nm and 70 nm AuNPs obtained at 80 kVp X-ray beam, 6 MV and 10 MV photon beam. In conclusion, AuNPs can be used during radiation therapy to kill cancer cells in order to reduce the dose of radiation to kill the tumours while at the same time sparing the normal tissue.

## **CHAPTER 1**

### **INTRODUCTION**

#### **1.0 Introduction**

This chapter contains an introduction and background to the radiotherapy that includes the statistics of breast cancer among worldwide and in Malaysia. The statistics highlight that more effective treatments are desperately needed, thus, one major concern in radiotherapy is the improvement in the distribution of the dose by delivering a sufficient dose to the cancer cells while at the same time sparing the healthy tissues are discussed in the problem statement of this study. The objectives of this thesis and the significance of study are also provided in this chapter. This chapter concludes with a description of the outline of this thesis.

#### **1.1 Background of Study**

Cancers figure among the leading causes of morbidity and mortality worldwide, with approximately 14 million new cases and accounting for 8.2 million deaths in 2012. Breast cancer is the most common cancer in women worldwide, with nearly 1.7 million new cases diagnosed in 2012 (second most common cancer overall), and leading cause of death worldwide, with a record 521 000 deaths (World Cancer Report, 2014). This represents about 12 % of all new cancer cases and 25 % of all cancer cases in women. The National Cancer Registry (NCR) 2003 - 2005

reported an age-standardised rate (ASR) of 47.3 per 100 000 population. This means that approximately 1 in 20 women in Malaysia develops breast cancer in their lifetime. However, the rate differs between the three main ethnics, in which the incidence is highest for Chinese (59.9 per 100 000 population), followed by Indians (54.2 per 100 000 population), and Malays (34.9 per 100 000 population) (Yip *et al.*, 2014). In 2006, there were 3525 breast cancer cases in female registered in NCR for that year, which accounted for 16.5 % of all cancer cases registered. The age pattern in 2006 showed a peak Age-specific Incidence Rate at the age group of 50 - 59 years old (Omar *et al.*, 2006). Moreover, the Penang Cancer Registry 2004 - 2008 reported an incidence of 48 per 100,000 population in Penang. The International Agency for Research in Cancer (GLOBOCAN) 2012 estimated the ASR of breast cancer in Malaysia as 38.7 per 100,000 population with 5410 new cases in 2012. Over the period of 12 years from 1993 to 2004, about 60 – 70 % of women presented early stage (Stages 1 - 2), while 30 - 40 % presented with late breast cancer (Stages 3 - 4). Malay patients present at later stages and with larger tumours. Consequently, their survival is worse than with Chinese and Indian women. The factors responsible for these ethnic differences are pharmacogenomics, lifestyle factors (such as weight-gain, diet and exercise), and psychosocial factors (such as acceptance of 2nd or 3rd line chemotherapy) (Yip *et al.*, 2006).

The statistics highlight that more effective treatments are desperately needed. In the recent years, the application of nanoparticles in diagnosis and treatment of cancer has been the issue of extensive research. Among these studies some have concentrated on the dose enhancement effect of gold nanoparticles (AuNPs) in radiation therapy of cancer. On the other hand, some studies indicated energy

dependency of dose enhancement effect, and the others have studied the AuNP size effect in association with photon energy. However, in some aspects of AuNP-based radiotherapy, the results of recent studies do not seem very conclusive, in spite of relative agreement on the basic physical interaction of photoelectric between AuNPs and low energy photons. The main idea behind the AuNP dose enhancement in some studies is not being able to explain the results, especially in recent investigation on cell lines and animal models radiation therapy using AuNPs.

Human breast tumour cell lines are needed for multidisciplinary research in breast cancer. However, there are few well-characterised cell lines derived from human mammary carcinomas. MCF-7 is a human breast cancer cell line that was first isolated in 1970 from the malignant adenocarcinoma breast tissue of a 69-year old woman. MCF-7 is the acronym of Michigan Cancer Foundation-7, referring to the institute in Detroit where the cell line was established. MCF-7 cells are useful for in vitro breast cancer studies because the cell line has retained several ideal characteristics particular to the mammary epithelium. These include the ability for MCF-7 cells to process estrogen via estrogen receptors. Moreover, MCF-7 cells are also sensitive to cytokeratin. When grown in vitro, the cell line is capable of forming domes and the epithelial like cells grow in monolayers.

Radiotherapy involves the use of X-rays, gamma rays, or charged particles, to deposit dose to treat and prevent the spread of the abnormal cancerous cells. Previous reports from Commonwealth and State agencies have pressed that slightly more than 50 % of all patients who developed cancer will require radiotherapy at some stage of their illness (Delaney *et al.*, 2003). Furthermore, radiotherapy has been used for

cancer treatments since the very end of the 19<sup>th</sup> century. When radiotherapy was first introduced, X-rays in the kV energy range were prescribed to treat cancerous tissues. This X-rays as in the kV energy range have low penetration, thus have a limited effect on deep-seated tumours. Besides, they have low skin sparing effect, in which they delivered high dose to the tissues in their path to the tumour and sometimes above the threshold (Bernier *et al.*, 2004). Major developments have recently been made to overcome this weakness, and within the last decade, electron linear accelerators machine (LINAC) has been introduced to generate higher energy X-rays and electron beams in MV range of energy for radiotherapy. LINAC is the most common source of ionising radiations and has been replacing kV and orthovoltage X-rays for use in clinical centres to deliver most forms of radiotherapy. However, one major concern in radiotherapy is the improvement in the distribution of the dose by delivering a sufficient dose to the cancer cells while at the same time sparing the healthy tissues.

## **1.2 Problem Statement**

One major concern in radiotherapy is the improvement in the distribution of the dose by delivering a sufficient dose to the cancer cells while at the same time sparing the healthy tissues. Technological progressive development in radiotherapy equipment has not only increased in penetrating power or expanded the range of beam energies that can be delivered to the patient, but also provided better tumour targeting while minimising radiation dose to the surrounding normal tissues.

Modern LINACs are able to perform sophisticated techniques such as stereotactic radiosurgery (SRS), image guided radiotherapy (IGRT), and intensity modulated radiotherapy (IMRT) that produce conformal dose to the tumours with high precision. However, the improvement of radiotherapy treatment in order to achieve maximum tumour control and reduce normal tissue complications not only depends on the advancement in technology and engineering, but also on an understanding of radiobiological science.

Altering tumour cell radiosensitivity with the goal to deliver sufficient radiation dose that can annihilate the tumours, without exceeding normal tissue tolerance may improve the whole radiotherapy treatment system. Radiosensitising agents or radiation dose enhancers may increase the effect of radiation to the tumour provided that the agents are able to be selectively targeted to cancer cells. Enhancing tumour radiosensitivity by increasing the cross section of radiation interaction in the tissue using high atomic number ( $Z$ ) materials has been explored over the last 20 years, typically using iodinated contrast agents (Rahman, 2010).

Enhancements of radiation effects by iodine were observed using many biological and phantom studies which proved the potential applicability of high  $Z$  materials as radiosensitisers (Cho & Krishnan, 2013). Moreover, this exploration has continued employing various high  $Z$  atoms and recent improvements in nanotechnology have made it possible to efficiently deliver large numbers of such high  $Z$  atoms to target regions. Among the many types of high  $Z$  nanoparticles which have been tested, such as silver and platinum, gold as a noble element was found to

be the most effective and biologically compatible. Metallic nanoparticles such as AuNPs appear to be promising as a radiosensitiser agent for radiotherapy.

Recently, the emerging nanotechnology field has created unprecedented potential for improving the outcome in cancer treatment using nanomaterials. Nanoparticles are typically smaller than several hundred nanometers in size, in the size range of large biological molecules such as enzymes, receptors and antibodies (Cai *et al.*, 2008). In this size range (approximately one hundred times smaller than human cells) nanoparticles can easily interact with biomolecules such as proteins and cellular structures.

The presence of AuNPs during radiotherapy, will enhance the radiation dose. The study by Kong *et al.* (2008) show that AuNPs only enhances the radiosensitivity of cancer cells, not in normal cells. In this study, we report that the nanometer size and high Z properties of AuNPs provide potential advantages in enhancing radiation dose to the tumour while preserving the surrounding normal tissue which is the ultimate goal in radiotherapy.

However, cancer therapy are facing tremendous opportunities and challenges in combining emerging nanotechnology with cellular and molecular techniques to develop better cancer diagnosis and therapeutic designs. Therapy combined with metallic nanoparticles is a new way to treat cancer, in which gold nanoparticles (AuNPs) are intravenously injected and contracted to tumour region. Then, when the



radiation interact with AuNPs, it will produce free radicals that will induce DNA damage and cell apoptosis to the cancer cells (Kong *et al.*, 2008).

### **1.3 Objectives**

The objectives of the study are:

1. To determine the IC<sub>50</sub> value of AuNPs to the breast cancer MCF-7 cells.
2. To measure the qualitative observation of the penetration of AuNPs into MCF-7 cells.
3. To determine the effects of AuNPs in MCF-7 cells treatment by X-ray and linear accelerator (LINAC).

### **1.4 Significance of Study**

Successful completion of the research will make possible to describe the nature of the gold nanoparticle toxicity. As a result of this research it will be possible to determine the effect of the enhancement of radiation effects by AuNPs on breast cancer MCF-7 cell line.

In current clinical practice, in which the dose of radiation is bound to sparing healthy tissue, this enhancement can be used to increase the therapeutic effects in

other advanced technologies in radiotherapy, such as intensity modulated radiation therapy (IMRT), image guided radiation therapy (IGRT), stereotactic body radiotherapy (SBRT), and adaptive radiation therapy (ART) by using kilovoltage superficial X-rays radiotherapy and megavoltage photon beam radiotherapy.

## **1.5 Outline of Thesis**

Chapter 1 is an introduction that include the background of study, problem statement, and objectives.. The significance of study are also explained.

Chapter 2 contains a detailed description of the gold nanoparticles (AuNPs), and the theoretical background of basic radiation physics, AuNPs radiation therapy in the kilovoltage range, interaction of radiation with AuNPs at the atomic level, and the AuNPs radiosensitisation. Review of previous and current work on radiation dose enhancement using high Z material, AuNPs and the AuNPs radiosensitisation in cell line (*in vitro*) and animal models (*in vivo*) are also provided.

Chapter 3 describes the general protocols for radiobiological study using cell culture. The protocols specify the characterization and preparation of AuNPs for biological study and basic cell culture protocol. Protocol for measuring AuNPs cytotoxicity and TEM analysis of cells with internalized AuNPs are also described. Besides, in this chapter, the cell irradiation methodology with kilovoltage superficial X-rays and megavoltage photon beam is explained.

Chapter 4 reports the results and discussions of the experiments which were conducted in the study. In this chapter, the results are divided into five parts which are characterisation of AuNPs, cell morphology analysis, cytotoxicity of AuNPs on MCF-7 cells, EFTEM analysis of MCF-7 cells with internalized AuNPs, and cell irradiation. The presence of AuNPs during irradiation of MCF-7 cells give the lower survival fraction of the cell. Means that more cells are found to be killed at the irradiation area containing AuNPs. More surprisingly, the obtained cell survival curves also lend a strong support to the argument that the size of AuNPs also plays important role in determine the enhancement radiation effects.

Chapter 5 is a conclusion of the study that include the recommendation for further work. Combination cancer therapy of X-rays and AuNPs will cause better tumour control compared to radiotherapy alone. In current clinical practice, in which the dose of radiation is bound to sparing healthy tissues, this enhancement can be used to increase the therapeutic effects in other advanced technologies in radiotherapy.

## **CHAPTER 2**

### **BACKGROUND, THEORY AND LITERATURE REVIEW**

#### **2.0 Introduction**

This chapter presents a theory and literature review of the properties of gold nanoparticles (AuNPs) as dose sensitizers. It includes an examination of the production of x-rays by conventional clinical modalities. Some radiation interaction processes at an atomic level and the effects of these interactions on the biological materials (targets) such as cells are illustrated. Basic radiobiology such as cell survival curve, linear energy transfer, and cell cycles effects are also described in this chapter to facilitate a better understanding of the damage caused by radiation.

#### **2.1 Gold Nanoparticles**

In the last fifteen years, the researcher were assisted to the massive advance of nanomaterials in material science. Every object possessing at least one characteristic dimension between 1 and 100 nm can be defined as a ‘nanomaterial’. When dealing with such small structures, the ratio between surface (or interface) and inner atoms became significant.

### 2.1.1 Synthesis

The approaches to metal nanoparticles synthesis can be divided in physical and chemical methods. Physical methods, as ion implantation and all the sputtering techniques, are used to obtain metal nanoparticles supported on substrates or embedded in solid matrices. Condensation of metal vapours by adiabatic expansion has been successfully exploited in the synthesis of metal particles as well as of oligoatomic metal clusters. The most widely used methods are based on chemical reduction in solution (wet chemistry) to yield nanoparticles colloids. Besides, all these wet chemical approaches require the reduction of  $\text{Au}^+$  ions and the chemisorption or physisorption of ligands on the surface of metal nanoparticles to avoid their coagulation and precipitation. The Turkevitch method is the most popular for obtaining aqueous solutions of gold nanoparticles that are easily functionalisable with subsequent steps. This method consists in the reduction of chloroauric acid,  $\text{HAuCl}_4$ , in a boiling aqueous solution of sodium citrate. The average particle diameter can be tuned in the range of 10 – 100 nm with limited polydispersity. Meanwhile, citrate molecules act both as reducing and stabilising agents (Amendola, 2008).

### 2.1.2 Chemical Properties

Gold is known for being generally inert and for not being attacked by  $\text{O}_2$  to a significant extent. This makes AuNPs stable in ordinary conditions. The AuNPs are resistant to a strong oxidising or a highly acid environments, though ‘aqua regia’ or

solution containing  $I^-$  or  $CN^-$  can immediately dissolve them. For instance, Au is reactive with sulphur. In case of organic thiols, ligation to nanoparticles surface is particularly effective for the contemporary presence of a  $\sigma$  type bond, in which metal electrons are partially delocalised in molecular orbitals formed between the filled  $d$  orbitals of the metal and the empty  $d$  orbitals of sulphur. Other than thiols and disulphides, alchilamine and phenilphosphine also have been successfully used for AuNP ligation. Other than that, electrochemical properties of metal nanoparticles are strongly size dependent, in fact cluster made by few hundred or tens of atoms has been used to investigate the transition from the metal – like capacitive charging to the redox like charging. Up to 15 charging peaks have been observed by differential pulse voltammetry in case of  $Au_{147}$ . In addition, high surface to bulk atoms ratio and overall chemical inertness confer catalytic activity to AuNP. AuNPs have been active in the oxidation of CO and  $H_2$  as well as in the reduction of NO and in a wide range of other typical catalytic reactions. Furthermore, AuNP has high chemical stability and photostability and non toxic for living organisms (Amendola, 2008).

### 2.1.3 Physical Properties

Since solid to liquid transition begins at interfaces, a well known feature of nanometric particles is the lower melting temperature with respect to the bulk. For instance, gold undergoes a decrease in melting temperature of about 400 °C, going from 20 nm to 5 nm particles and of about 50 °C going from the bulk to 20 nm particles. The melting temperature,  $T_m$  depends on particle size,  $d$  as:

$$T_m = A + \frac{B}{d} \quad (2.1)$$

where A and B are two constants.

A general rule for physical properties dependent on the surface to volume ratio, can be described by using the ‘size equations’ structure as in Equation (2.1). Thermal conductivity is enhanced for small particles due to higher surface to volume ratio, while phonons energy becomes higher for very small particles and Raman spectroscopy can be used to measure clusters size. Another surface phenomenon is the plasmon – polariton absorption band due to the coherent oscillation of  $6S^1$  (Au) conduction band electrons in presence of resonant electromagnetic waves. For spherical AuNP with diameter 2 and 100 nm, the position of this surface plasmon absorption (SPA) is about 520 nm. This plasmon oscillation, namely the displacement of conduction electrons from their equilibrium positions around positive ionic core, produces strong electric fields on particles surface, with intensity depending on their shape and assembly. In this case a size equation is used to describe the damping of the SPA band. In general, plasmon oscillations have a fast damping times also for bigger sizes, as apparent for the intrinsic width of SPA. Furthermore the SPA relaxation is essentially nonradiative. This make AuNP an efficient localised converter of visible wavelengths into heat (Amendola, 2008). A surface is directly connected to the underlying bulk, which means that the properties of the bulk material will most probably influence the properties and behaviour of the surface. Table 2.1 shows the bulk properties of gold.

**Table 2.1** Bulk Properties of Gold Nanoparticles

<b>Bulk Properties</b>	<b>Gold</b>
Electronic Configuration	[Xe] 5d <sup>10</sup> 6s <sup>1</sup>
Atomic Number – Weight	79 – 196.97 u.a.
Lattice	f.c.c.
Lattice Parameter	0.408 nm
Density	19.28 g cm <sup>-3</sup>
Atomic Density	59 nm <sup>-3</sup>
Volume for Atom	0.017 nm <sup>3</sup>
Wigner – Seitz Radius	0.159 nm
Electronic Density	5.90 x 10 <sup>28</sup> m <sup>-3</sup>
Fermi Speed	1.40 x 10 <sup>8</sup> cm s <sup>-1</sup>
Fermi Energy	5.51 eV
Plasma Frequency	1.31 x 10 <sup>16</sup> rad s <sup>-1</sup>
Relaxation Time	2.94 x 10 <sup>-14</sup> s
Ionization Energy	9.22 eV
Electric Resistivity	2.20 x 10 <sup>-6</sup> Ω cm
Melting Temperature	1338 K
Boiling Temperature	3243 K
Thermal Conductivity	3.17 W cm <sup>-1</sup> K <sup>-1</sup>
Heat Capacity	(25 °C) 25.418 J mol <sup>-1</sup> K <sup>-1</sup>
Standard Potential	+1.69 V
Electronegativity	2.4



## 2.2 Basic Radiation Physics

Nanoparticles are defined as microscopic particles between 1 to 100 nm, with at least two dimensions. Its distribution within the body is based on various parameters, such as their relatively small size resulting in longer circulation times, and their ability to take advantage of tumor characteristics (Praetorius & Mandal, 2007). Furthermore, in cancer treatment, these nanoparticles have provided better penetration ability of substances used for therapy and diagnosis with lower risk compared to conventional drugs (Porcel *et al.*, 2010). Nanoparticles distribution is influenced by different parameters, like size and their ability to use cancerous cells features for own inactivation (Brun *et al.*, 2009).

Radiation therapy with ionising radiations including X-rays, gamma rays, and high energy particles is employed extensively for treatment of almost all types of solid tumours. For instance, radiation is the emission of matter or energy. There are many forms of radiation, such as, light is a visible form of radiation, heat is another form of radiation, and X-rays from an imaging or therapy machine are also radiation. X-rays are produced by two different mechanisms, one gives rise to bremsstrahlung X-rays and the other characteristic X-rays. X-rays have several basic properties which are unaffected by gravity, electric fields, and magnetic fields. It can travel in straight lines, exponentially attenuated by matter, and cannot be focused.

The process of bremsstrahlung (braking radiation) is the result of radiative interaction between a high-speed electron and an atomic nucleus. The electron while

passing nearby a nucleus may be deflected from its path by the action of Coulomb forces of attraction and lose energy as bremsstrahlung. According to Maxwell's general theory of electromagnetic radiation, as the incoming high speed electron passes through the nucleus, it will deflect and a part of its energy will propagate through space as electromagnetic radiation. The mechanism of bremsstrahlung production is illustrated in Figure 2.1.

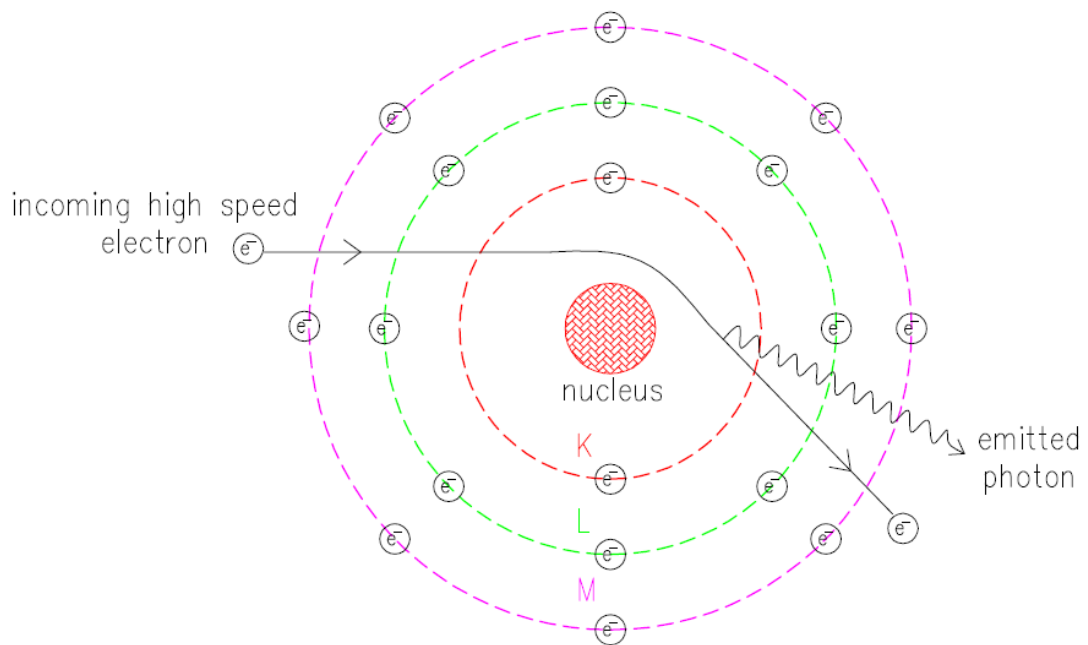


**Figure 2.1** Mechanism of bremsstrahlung process.

The incoming high speed electron may have one or more bremsstrahlung interactions. This interaction either causes a partial or complete loss of electron energy. So, the bremsstrahlung photon results from this interaction may have energy up to the initial energy of the electron. Besides, the energy of the incoming high speed electrons will determine the direction of emission of the bremsstrahlung photons.

Electrons incident on the target also produces characteristic of X-rays. The mechanism of characteristic radiation production is illustrated in Figure 2.2. When an electron, with kinetic energy  $E_0$ , interact with the atom of the target, it will eject an orbital electron, such as a K, L, or M electron, and leave the atom ionized. The original electron will recede from the collision with energy  $E_0 - \Delta E$ , where  $\Delta E$  is the energy given to the orbital electron. A part of  $\Delta E$  is spent in overcoming the binding energy of the electron and the rest is carried by the ejected electron. When there is a vacancy in an orbit, an outer orbital electron will fall down to fill that vacancy, and the energy is radiated in the form of electromagnetic radiation. This is called characteristic radiation, characteristic of the atoms in the target and of the shells between which the transitions took place.

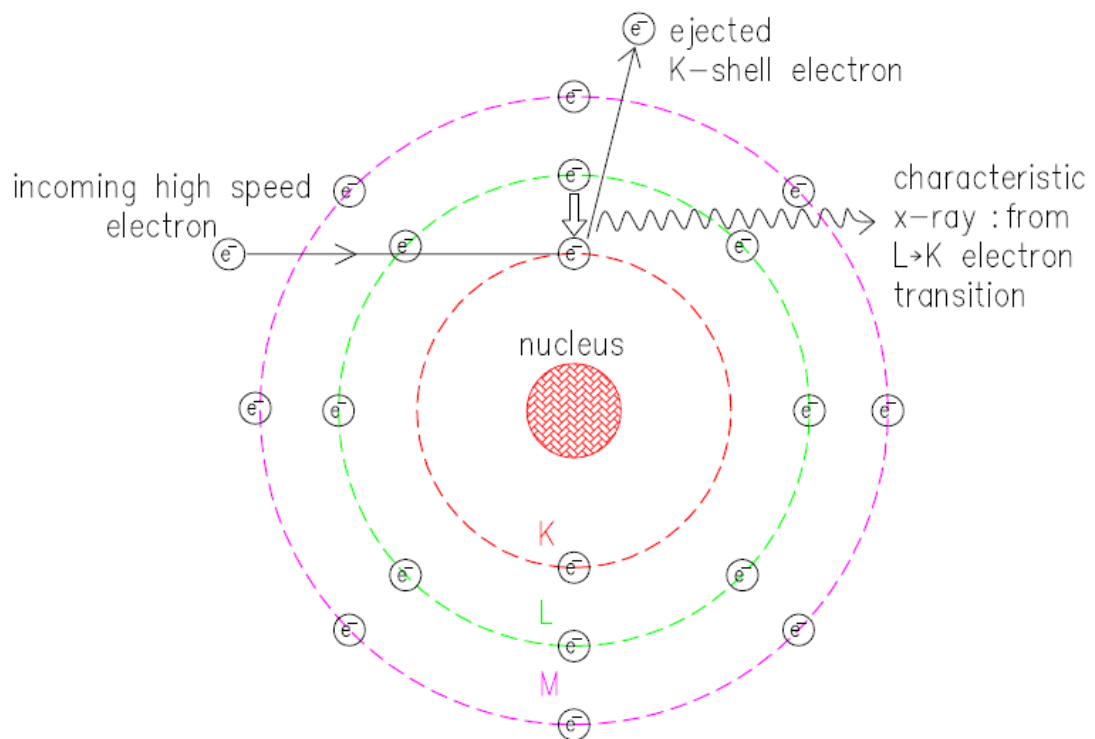


**Figure 2.2** Mechanism of characteristic X-ray.

The characteristic radiations emitted are of high enough energies to be considered in the X-ray part of the electromagnetic spectrum. Characteristic radiation is unlike the bremsstrahlung radiation, X-rays are emitted at discrete energies. When the electron from the L shell fill the vacancy at the K shell, the energy of the emitted photon is equal to the energy of binding electron of the K shell minus the energy of binding electron of the L shell.

### **2.3 AuNPs Radiation Therapy in the Kilovoltage Range**

Ionising radiations do not discriminate between cancerous and normal cells. Thus, normal tissue damage is still the dose limiting factor that diminishes tumour cells eradication in radiation therapy. Application of tumour-specific nanoparticles in radiation therapy has aimed to improve the radiation therapy outcomes by inducing more toxicity for tumours and less for normal tissues. Among various nanoparticles, preclinical studies have reported gold nanoparticles (AuNPs) radiosensitisation effect in conjunction with different photon beams. According to the National Council on Radiation Protection (NCRP Report No. 33, 1968), X-ray therapy in the kilovoltage range is divided into subcategories based on the beam quality and their use as shown in Table 2.2.

Although Monte Carlo (MC) simulations of AuNPs have demonstrated physical dose enhancement of about 60 % for X-rays in kV range and low energy photons from  $^{192}\text{Ir}$  brachytherapy sources (Zhang *et al.*, 2009), the biological study of Jain *et al.* (2011) found comparable sensitization effect at kilovoltage and

megavoltage X-ray energies (Mousavie *et al.*, 2013). It was also suggested that physical dose enhancement based on increased X-ray absorption could not be the main mechanism of sensitisation. However, it should be noted that the used AuNP dimensions have been different. In the Monte Carlo study, the AuNPs with diameter of 100 nm were used, while in the biological study the diameter of 1.9 nm were used. In the pioneering study of Heinfeld *et al.* (2004), the AuNP with the diameter of 1.9 nm was injected intravenously into mammary tumour-bearing mice in combination with 250 kVp X-ray (Hainfeld *et al.*, 2004). Results showed a 86 % one-year survival for new method compared to 20 % for X-rays alone.

**Table 2.2** Subcategories of the X-ray therapy in the kilovoltage range based on the beam quality and their use (Khan, 2003).

<b>Subcategories of the X-ray therapy in the kilovoltage range</b>	<b>The energy of the X-rays beam (kVp)</b>
Grenz-Ray	< 20
Contact	40 to 50
Superficial	50 to 150
Orthovoltage	150 to 500
Supervoltage	500 to 1000
Megavoltage	$\geq 1\ 000$

Another study was conducted by Chang *et al.* (2008) on melanoma tumor-bearing mice using 13nm AuNP in conjunction with a single dose of 25 Gy of 6MeV electron beam. It resulted in significant reduction in tumor volume compared to a

control group. Additionally, the number of apoptotic cells in AuNP plus irradiation animals was two times higher than irradiation alone. It is believed that interactions of X-rays and AuNP result in the release of photoelectrons. Moreover, the range of these electrons is very short relative to photons and a pronounced energy is deposited in cells containing AuNP or in direct proximity to gold atoms. The controversial results concerning AuNP radiosensitisation could be originated from the differences in performed investigations in terms of key parameters including AuNP shape, size, concentration and type of cell lines, and radiation energy and type. To address the problem, the affecting parameters in AuNP X-ray radiosensitisation were comprehensively evaluated by Brun *et al.* (2009). In the present review, the principles behind the AuNP radiosensitisation are discussed and the results of the related studies are reviewed.

#### **2.4 Interaction of Radiation with AuNPs at the Atomic Level**

The radiation interaction with AuNPs on the cellular level and its molecular partners in biochemical reactions and the subsequent mechanisms which lead to dose enhancement is one of the important theoretical principles to be discussed further for clinical application of AuNP-based radiation therapy.

The study by Zhang *et al.* (2009) examines the cytotoxicity of AuNPs and stability of the radiation for radiotherapy purposes. The findings indicate that there is no obvious instability and size variation in spherical AuNPs with the diameter of 15 nm following gamma radiation of 2 000 – 10 000 Rontgen. The main point is the

cytotoxicity results showed that the extremely high concentration of AuNP could cause a sharp drop off in K562 cell viability, while the low concentration did not affect the cell viability (X.-D. Zhang *et al.*, 2009). When photons pass through a material, they may be transmitted through the material without interaction, or may be attenuated by absorption or scattering processes (Khan, 2003 ; Cho & Krishnan, 2013).

#### 2.4.1 Coherent Scattering

The first physical interaction is coherent scattering which is also known as classical scattering or Rayleigh scattering. Coherent scattering is the process by which the incident photons are scattered without losing energy and the wavelength of the scattered photon is the same as the wavelength of the incident photon. In this interaction, the incident photon passing near the atom's electron, usually the electron in the outermost shell, and setting it into oscillation as shown in Figure 2.3.

The oscillating electron reradiates the energy at the same frequency and phase as the incident electromagnetic wave and the only effect is the scattering of the photon at small angles. Unfortunately, coherent scattering plays no role in radiation therapy because it is probable in high atomic number materials and with photons of low energy, but there is no deposition of energy in the medium.

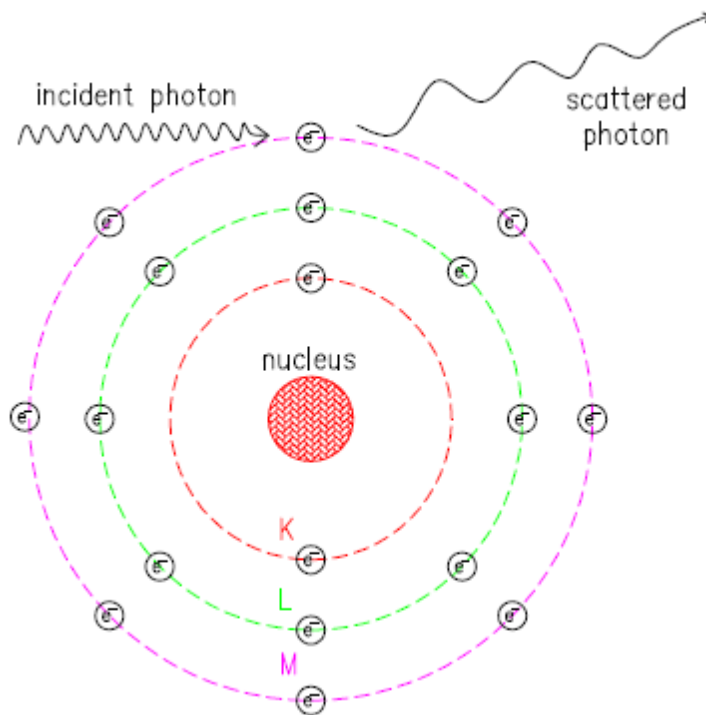


**Figure 2.3** Mechanism of coherent scattering.

#### 2.4.2 Photoelectric Effect

The photoelectric effect is the predominant process for photons with energy from 10 to 500 keV. For instance, the photoelectric effect is a phenomenon in which an incident photon interacts with an atom and ejects one of the orbital electrons from the atom as shown in Figure 2.4. After the electron has been ejected from the atom, a vacancy is created in the K, or L shell, thus leaving the atom in an excited state. The vacancy can be filled by an outer orbital electron, results in a de-excitation of the atomic system, either by characteristic X-ray or Auger-electron emission. The result of this process is the production of electrons (also called as photoelectron), characteristic X-ray of gold atoms or auger electrons.



The entire energy  $h\nu$  of the photon in this process is first absorbed by the atom and then transferred to the atomic electron. The kinetic energy of the photoelectron is equal to  $h\nu - E_B$ , where  $E_B$  is the binding energy of the electron. The relative probability of these de-excitation processes is given by the fluorescence yield which is strongly dependent on atomic number ( $Z$ ), being small for light atoms and large for heavy atoms such as gold. For instance, AuNPs are based on high- $Z$  materials. However, the Auger effect not be a major contributor to the dose deposited in the presence of high- $Z$  NPs, because it is more concerned for low- $Z$  NPs. In fact, Auger effect is dominant for  $Z$  less than 15 but almost equal to 0 for  $Z$  more than 60 (Retif *et al.*, 2015).

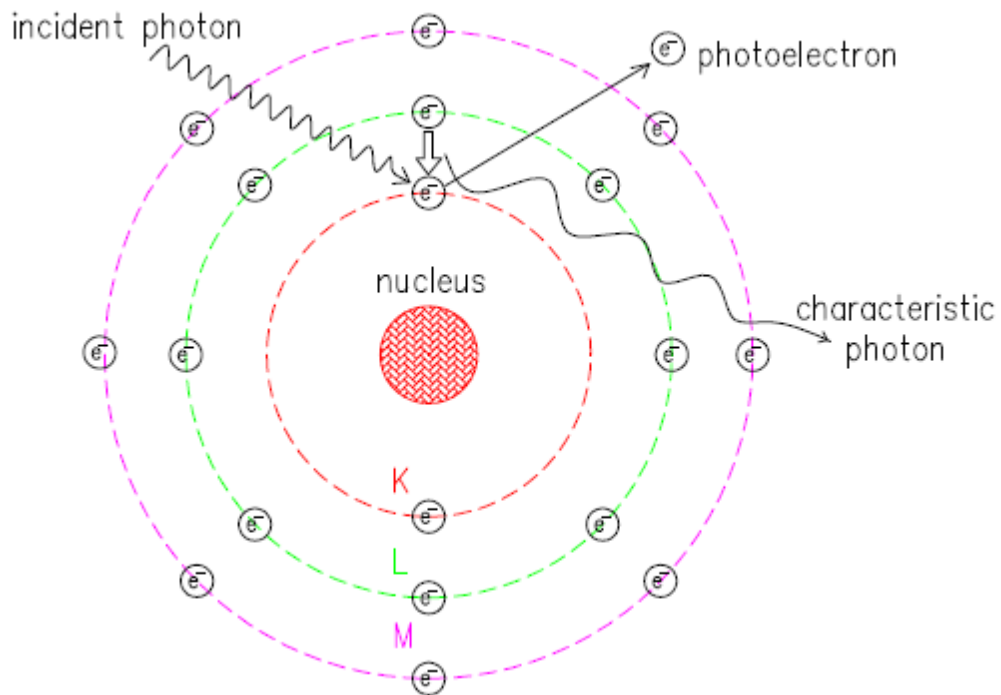


**Figure 2.4** Mechanism of photoelectric effect.

### 2.4.3 Compton Scattering

In addition, for photons above 500 keV, the Compton scattering and excitation is observed. In the Compton process, the photon interacts with an atomic electron as though it was a “free” electron (binding energy of the electron is much less than the energy of the bombarding photon) and will result in production of Compton electrons due to the re-excitation of the atom, which leads to photoelectric effect as shown in Figure 2.5. In this interaction, the electron receives some energy from the photon and is emitted at an angle  $\theta$  as illustrated in Figure 2.5. The photon, with reduced energy, is scattered at an angle  $\phi$ .

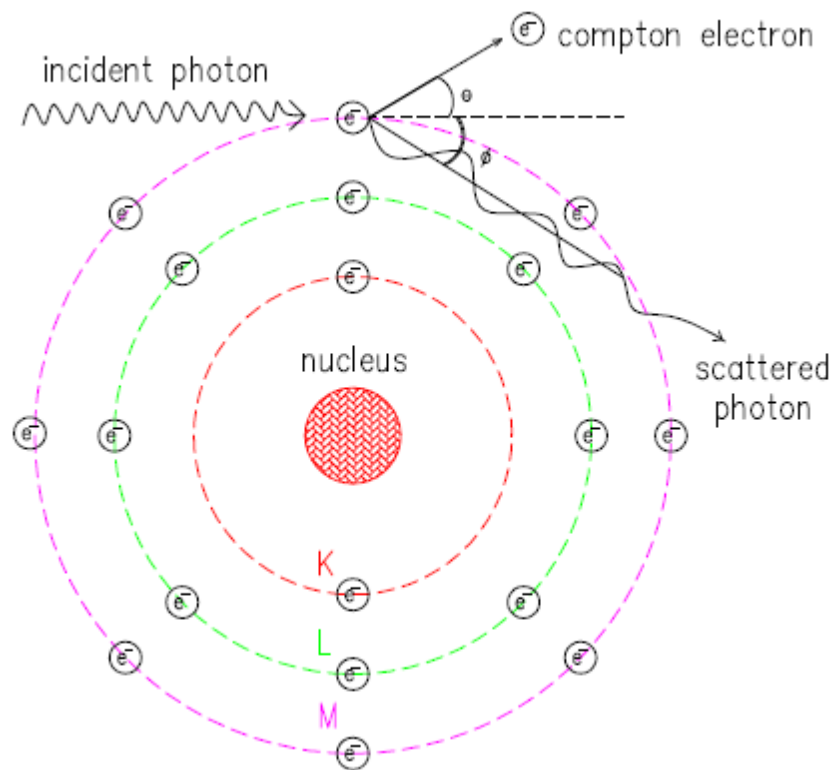


**Figure 2.5** Mechanism of compton effect.